ANNALS of Clinical and Translational Neurology
Open Access
AMERICAN NEUROLOGICAL ASSOCIATION

RESEARCH ARTICLE

The potassium channel Kv1.3 as a therapeutic target for immunocytoprotection after reperfusion

Yi-Je Chen[1,2], Yanjun Cui[1], Latika Singh[1] & Heike Wulff[1]

[1]Department of Pharmacology, School of Medicine, University of California, Davis, California 95616
[2]Animal Models Core, Department of Pharmacology, School of Medicine, University of California, Davis, California 95616

Correspondence
Heike Wulff, Department of Pharmacology, School of Medicine, University of California, Davis; 451 Health Sciences Drive, GBSF 3502, Davis, CA 95616. Tel: +1-530-754-6135; Fax: +1-530-752-7710; E-mail: hwulff@ucdavis.edu

Funding Information
This work was supported by the National Institute of Neurological Disease and Stroke (NS100294 to H.W.). The authors thank the staff of the UC Davis Mouse Biology program. This resource was funded by the UC Davis Comprehensive Cancer Center Support Grant (CCSG) awarded by the National Cancer Institute (NCI P30CA093373).

Received: 23 July 2021; Revised: 3 September 2021; Accepted: 7 September 2021

Annals of Clinical and Translational Neurology **2021; 8(10): 2070–2082**

doi: 10.1002/acn3.51456

Abstract

Objective: The voltage-gated potassium channel Kv1.3, which is expressed on activated, disease-associated microglia and memory T cells, constitutes an attractive target for immunocytoprotection after endovascular thrombectomy (EVT). Using young male mice and rats we previously demonstrated that the Kv1.3 blocker PAP-1 when started 12 h after reperfusion dose-dependently reduces infarction and improves neurological deficit on day 8. However, these proof-of-concept findings are of limited translational value because the majority of strokes occur in patients over 65 and, when considering overall lifetime risk, in females. Here, we therefore tested whether Kv1.3 deletion or delayed pharmacological therapy would be beneficial in females and aged animals. **Methods**: Transient middle cerebral artery occlusion (tMCAO, 60 min) was induced in 16-week-old and 80-week-old male and female wild-type C57BL/6J and Kv1.3$^{-/-}$ mice. Stroke outcomes were assessed daily with the 14-score tactile and proprioceptive limp placing test and on day 8 before sacrifice by T2-weighted MRI. Young and old female mice were treated twice daily with 40 mg/kg PAP-1 starting 12 h after reperfusion. Microglia/macrophage activation and T-cell infiltration were evaluated in whole slide scans. **Results**: Kv1.3 deletion provided no significant benefit in young females but improved outcomes in young males, old males, and old females compared with wild-type controls of the same sex. Delayed PAP-1 treatment improved outcomes in both young and old females. In old females, Kv1.3 deletion and PAP-1 treatment significantly reduced Iba-1 and CD3 staining intensity in the ipsilateral hemisphere. **Interpretation**: Our preclinical studies using aged and female mice further validate Kv1.3 inhibitors as potential adjunctive treatments for reperfusion therapy in stroke by providing both genetic and pharmacological verification.

Introduction

Stroke is the leading cause of long-term disability and currently the fifth most common cause of death in the United States after heart disease, cancer, respiratory diseases, and injuries/accidents.[1] While intravenous thrombolysis (IVT) with fibrinolytic drugs and/or endovascular thrombectomy (EVT), have significantly improved outcomes, there still is a need to identify what has recently been termed "brain cytoprotectants" as adjunctive treatments to reperfusion therapy by the Stroke Treatment Academic Industry Roundtable (STAIR) X.[2] EVT can achieve complete or near-complete recanalization in over 80% of patients with large vessel occlusions[3] and is increasingly employed beyond the traditional 6-hour time window with positive outcomes if imaging identifies salvageable tissue.[4,5] In this reperfusion era, it has been suggested to search for therapeutic approaches that could either "freeze" the penumbra[6] before EVT or ameliorate the consequences of reperfusion injury by the administration during or after thrombectomy.[2,7]

One approach that might be particularly attractive to consider as an adjunctive is immunomodulatory drugs that could ameliorate the secondary inflammatory damage resulting from microglia activation and immune cell infiltration.[8–10] However, immunomodulatory drugs used in

the wake of stroke should not produce general immunosuppression and thus aggravate the increased post-stroke risk of urinary and respiratory tract infections[11] but rather preferentially target pro-inflammatory, detrimental microglia, and lymphocyte functions without compromising beneficial immune functions.[9,10] A pharmacological target that fulfills these criteria is the voltage-gated potassium channel Kv1.3, which is widely expressed in the immune system[12] and upregulated on effector memory T cells[13] as well as on classically activated pro-inflammatory,[14,15] disease-associated microglia.[16] Inhibition of Kv1.3 with the brain penetrant small molecule PAP-1 reduces inflammation and pathology and improves behavioral outcomes in animal models of Alzheimer's disease, Parkinson's disease, and postoperative cognitive decline.[17–19] While there are, of course, many immunosuppressive drugs that can reduce neuroinflammation, what sets Kv1.3 blockers aside is that they are mild immunomodulators that do not induce lymphopenia,[13,20] delay wound healing,[19] or affect the ability of rats to clear influenza and *Chlamydia* infections or prevent rhesus macaques from developing protective, flu-specific central memory T-cell responses following intranasal immunization with a live influenza vaccine.[21,22]

We previously demonstrated that PAP-1 dose-dependently reduces infarction, improves neurological deficits, and reduces brain levels of IL-1β and IFN-γ while not affecting phagocytosis of neuronal debris or levels of IL-10 and brain-derived nerve growth factor in an ischemic stroke model in young male mice.[23] We here set out to test our therapeutic hypothesis that Kv1.3 constitutes a target for immunocytoprotection as an adjunctive to stroke reperfusion therapy by (1) confirming our previous pharmacological observations through genetic deletion of the channel and (2) by testing whether Kv1.3 deletion or delayed pharmacological therapy would be beneficial in females and aged animals. To simulate EVT and its resulting reperfusion effects we are using 60 min of transient middle cerebral artery occlusion followed by 8 days of reperfusion in mice, a model that is considered a relevant small animal model for EVT.[2,24]

Materials and Methods

Animals and housing

This study was approved by the University of California, Davis, Animal Use and Care Committee and conducted in accordance with guidelines for survival surgery and the IMPROVE guidelines for ischemic stroke in rodents.[25] Adult male and female C57BL/6J mice were purchased from Jackson Laboratory (stock number: 000664) at 14 or 72–75 weeks of age, acclimatized to the vivarium, and used for surgery when they were 16 or 80 weeks old. Kv1.3$^{-/-}$ mice on the C57BL/6J background[26] were a gift from Dr. Leonard Kaczmarek at Yale University and were rederived onto the C57BL/6J background to homozygosity by the Mouse Biology Program (https://mbp.mousebiology.org/) at UC Davis. Adult mice were transferred out of the barrier vivarium after weaning and aged in a campus vivarium. Mice were group housed in filtertop cages with an enriched environment (shredded paper in paper bags) under a 12-h light/dark cycle. Males and females were housed in separate cages but, whenever possible, in groups of 2–4 before and after surgery. Animals had ad libitum access to standard chow and water. Room temperature and humidity were monitored and kept at 22 ± 1°C and 50% ± 10%. After surgeries, soft water-soaked chow was provided in the cages.

Filament induce temporal middle cerebral artery occlusion

Reversible focal cerebral ischemia was induced by occlusion of the left middle cerebral artery (MCA) according to the classic filament method of Zea Longa[27] as previously described by us for male mice.[23] All surgeries were performed between 8 and 12 AM in the Microsurgery Core of the UC Davis School of Medicine by a microsurgeon with 20 years of experience. Anesthesia was induced with 5% isoflurane and then maintained with 0.5%–1.5% isoflurane in medical pure oxygen administered through a facemask. To assure consistent and continuous reduction of cerebral blood flow (CBF), a laser Doppler (Moor Instruments: MOORVMS-LDF) probe adapter was affixed to the surface of the skull over the area supplied by the MCA and secured in position by applying medical adhesive and dental cement to the base and around the edges of the adapter. The probe remained in place throughout the surgery and CBF was measured continuously to confirm occlusion and later establishment of reperfusion. Under a surgical microscope, the left common carotid artery (CCA) was exposed through blunt dissection and a ventral midline neck incision. The digastric, sternomastoid, and omohyoid muscles were retracted using metal hooks. Following isolation of the internal carotid artery (ICA) and the external carotid artery (ECA) from surrounding tissue and being ligated, the CCA and ICA were temporarily clamped using microvascular clips, to allow insertion of silicone rubber-coated nylon monofilament with a tip diameter of 0.21 ± 0.02 mm (No. 702112PK5Re, Doccol Corporation) through the ECA. The ECA was dissected and the Doccol filament was loosely secured inside the ECA using a 6-0 silk suture. This allowed gentle movement of the filament into the ICA and the eventual occlusion of the MCA. Animals

were kept under anesthesia and body temperature was monitored throughout the whole procedure and maintained at ≥36.5°C using a feedback-controlled heating pad. Following 60 min of MCAO, the filament was withdrawn to allow reperfusion. Blood flow measurements were continued for another 15 min before removing the adapter and the laser Doppler probe. The skin incision was closed using sterile skin staplers and the animals were allowed to recover from anesthesia in the surgery room on a heating blanket and returned to the vivarium when they were fully awake. Animals received subcutaneous Buprenex at 0.02 mg/kg every 12 h to limit post-surgical pain for 24 h after surgery.

Four MCAO surgeries were performed per day. The survival rate was 85% in 16-week-old animals and 75% and 71%, respectively, in aged males and females. Animals where CBF was not reduced by at least 70% and which did not display any obvious neurological deficit with a neuroscore of 1–2 at 12 h after reperfusion were excluded. Out of the animals surviving to day 8 (124 out of 145), 3 animals were excluded due to insufficient occlusion and insufficient neurological deficit. Animals that met these inclusion criteria were assigned to treatment or vehicle groups based on a computer-generated randomization scheme. Using our previous work,[23] where 11 animals per group allowed us to detect a ~50% reduction in infarct area, to provide conservative mean and standard deviation parameter estimates, sample size was powered to detect a reduction of 40% in mean percentage infarct area with 80% power. Using G*Power 3.1.7 to estimate the power for a pairwise contrast in means between independent groups, our statistical support determined that 10 animals per group would provide 82.3% power and 13 animals per group would provide 91.6% power, under two-sided testing with $\alpha = 5\%$. With our group sizes varying between 9 and 15 we therefore presumably had at least 80% power for every comparison. All animals were treated with vehicle (see below) to allow comparisons to PAP-1-treated animals.

PAP-1 treatment

Starting 12 h after reperfusion and following the first neurological scoring animals received the vehicle Miglyol 812 neutral oil (Neobee M5®, Spectrum Chemicals) or PAP-1 at 40 mg/kg intraperitoneally every 12 h until sacrifice on day 8. Miglyol 812 is a low viscosity oily vehicle, which is widely used as an excipient and well tolerated for i.p., s.c., or oral administration. It can be autoclaved and allows for the dissolution of lipophilic compounds at high concentrations (20 mg/mL for this study). PAP-1 was synthesized in our laboratory[28] and chemical identity and purity were tested by ^{1}H- and ^{13}C-NMR, high-resolution mass spectrometry, and UPLC/MS.

Neurological scoring

Since filament MCAO induces infarction not only in the major MCA territory, the lateral and parietal cortex, but also in the striatum we used the 14-score tactile and proprioceptive limp placing test[29] to evaluate mice every 24 h. MCAO severely affects sensorimotor coordination in this test, in which a normal mouse scores 14, while mice subjected to MCAO typically exhibit scores of ~1 when tested 12 h after surgery. Proprioception, forward extension, lateral abduction, and adduction were tested with vision (forelimb) or tactile stimuli (forelimb and hind limb). For visual limb placing, mice were held and slowly moved forward or lateral toward the top of a table. Normal mice placed both forepaws on the tabletop. Tactile forward and lateral limb placing were tested by lightly contacting the table edge with the dorsal or lateral surface of a mouse's paw while avoiding whisker contact and covering the eyes to avoid vision. For proprioceptive hind limb placing, animals were pushed along the edge of an elevated platform to test proprioceptive hind limb adduction. The paw was pulled down and away from the platform edge, and the ability to retrieve and place the paw on the surface upon sudden release was assessed. For each test, limb placing scores were 0 = no placing; 1 = incomplete and/or delayed (>2 sec) placing; or 2 = immediate and complete placing. For each body side, the maximum summed visual limb placing score was 4 and the maximum summed tactile and proprioceptive limb placing score, including the platform test, was 14. The investigator performing the neurological scoring was blinded to the treatments or genotype of the mice.

Assessment of infarct area by MRI

Infarct volume on day 8 was evaluated with T2-weighted MRI imaging in the Nuclear Magnetic Resonance (NMR) Facility at UC Davis. MRI was performed with a 7T (300 MHz) Bruker Biospec MR system running ParaVision version 5. The RF coil was Bruker's standard 35 mm ID mouse whole body resonator. Animals were anesthetized with isoflurane and placed on a heated circulating water blanket (37°C) to maintain body temperature. Fast spin echo (FSE) imaging, also known as RARE (Rapid Acquisition with Relaxation Enhancement) sequence, was used to acquire tri-pilot geometry reference images. The multi-slice multi-echo (MSME) sequence (TE:56 msec; TR: 1681.2 msec) was used to acquire images of seven coronal sections with 1-mm thickness from the junction of olfactory bulb and cortex. The

infarct area was analyzed with Adobe Photoshop CS6 by an investigator blinded to the treatments and genotypes. The percentage of infarcted area was calculated with the equation: (Infarct Area ÷ Ipsilateral Hemisphere Area) × 100%.

Immunohistochemistry

After the MRI on day 8, animals were euthanized with an overdose of isoflurane, brains quickly removed, and sectioned into four 2-mm thick coronal slices starting from the frontal pole. Slices were fixed in 10% buffered formalin for 24 h and then stored in 70% ethanol before being embedded in paraffin and sectioned at 5 μm by the Histology Laboratory of the UC Davis School of Veterinary Medicine. Following antigen retrieval (heating in 10 mmol/L Na citrate for 15 min in a microwave) the 4-mm and the 6-mm sections were stained with polyclonal rabbit antibodies for Iba-1 (1:3000, 019-19741 from Wako) and for CD3 (1:600, A045201-2 from Dako). Bound primary antibodies were detected with a Biotin-SP-conjugated goat anti-rabbit antibody (1:250, 111-065-144 from Jackson ImmunoResearch) and staining intensity amplified with the Vectastain Elite ABC Kit (Vector Laboratories). For the analysis of Iba-1$^+$ and CD3$^+$ cells, the whole 4-mm and 6-mm section of each animal was photographed in the brightfield channel on a Keyence BZ-X710 fluorescence microscope in the "stitching mode" with the 20x lens (exposure time 1/200s). The images were then exported from the BZ-X analyzer as "tiff" files and analyzed in Adobe Photoshop CS6. The entire infarcted hemisphere was outlined using the "Magnetic Lasso" tool. The "Magic Wand" was used to determine the number of total and positively stained pixels in the hemisphere. Artifacts or cracks were subtracted. Results are reported as percentage of positive pixels in the infarcted hemisphere.

The immunofluorescence staining in Figure 2 was performed with a polyclonal guinea pig anti-Kv1.3 antibody (1:100, AGP-005 from Alomone Labs) and the same polyclonal rabbit Iba-1 (1;1000) and CD3 (1:250) antibodies listed above; Secondary Abs: Alexa Fluor®546-goat anti-guinea pig IgG (1:1000, ab150185 from Abcam) and Alexa Fluor®488-goat anti-rabbit IgG (1:1500, ab150077 from Abcam).

Statistics analyses

Statistical analysis of infarct area and neurological deficit scoring comparing two groups (e.g., male vs. female or WT vs. Kv1.3$^{-/-}$ mice) was performed with unpaired *t*-test (Origin software). All data are shown as whisker plots with an overlay of the individual animal data. The boxes show mean ± SEM and the whiskers show confidence intervals. For the IHC data in Figure 5 comparing three groups one-way ANOVA (Origin software) followed by *post hoc* pairwise comparison of the different groups using Tukey's method was used as recommended by Schlattmann and Dirnagl for MCAO studies.[30] $p < 0.05$ was used as the level of significance. *$p < 0.05$, **$p < 0.01$, ***$p < 0.001$.

Results

Establishment of tMCAO in female and aged 80-week-old mice

Since we had previously only performed MCAO in young male mice and rats,[23] we first established reversible focal cerebral ischemia induced by 60-min occlusion of the left MCA in female C57BL/6J mice. Initial pilot surgeries revealed that it was difficult to achieve a good survival rate with 12-week-old female mice because the smallest size available Doccol filament occluded too well and we therefore used 16-week-old animals to compare males and females, who at this age both exhibited a survival rate of 85% with 70%–85% occlusion for 60 min in our hands. In keeping with literature[31] we found that young females exhibited smaller infarcts as measured by T2-weighted MRI on day 8 and a milder neurological deficit than males on the 14-score system starting from day 4 onward (Fig. 1A, Table S1). In contrast to young females, 80-week-old females exhibited infarct areas and neurological deficit scores in our hands that were comparable to 80-week-old males (Fig. 1B) and significantly more severe than in young females. The daily evolution of body weight and a comparison of young versus old animals of the same sex are provided in Figures S1 and S2. These observations are in agreement with previous reports of smaller infarcts in 5-month-old cycling than in 20-month-old (= 80 weeks) anovulary and persistently acyclic female C57BL/6 mice due to the protective effects of estrogen in young females.[31]

Since there are reports about potential stroke therapeutics like minocycline or splenectomy only benefiting males, or of targets like P2X4 being differentially expressed in females versus males, we next investigated if Kv1.3 expression increases in both sexes following ischemic stroke. In male mice, we had previously observed increasing Kv1.3 immunoreactivity between day 2 and the peak of microglia activation on day 8.[23] When using heterozygous CX3CR1$^{+/GFP}$ mice for tMCAO surgery we observed similarly intense Kv1.3 staining on day 8 in the brains of both sexes that localized to the infarct area outlined by the strongly GFP-fluorescent CX3CR1 expressing cells (Fig. S3). Patch-clamp studies performed on acutely isolated CD11b$^+$ cells from the infarcted hemisphere showed similar Kv1.3 current densities in male and female mice.[32] At 16 weeks of age, WT females have

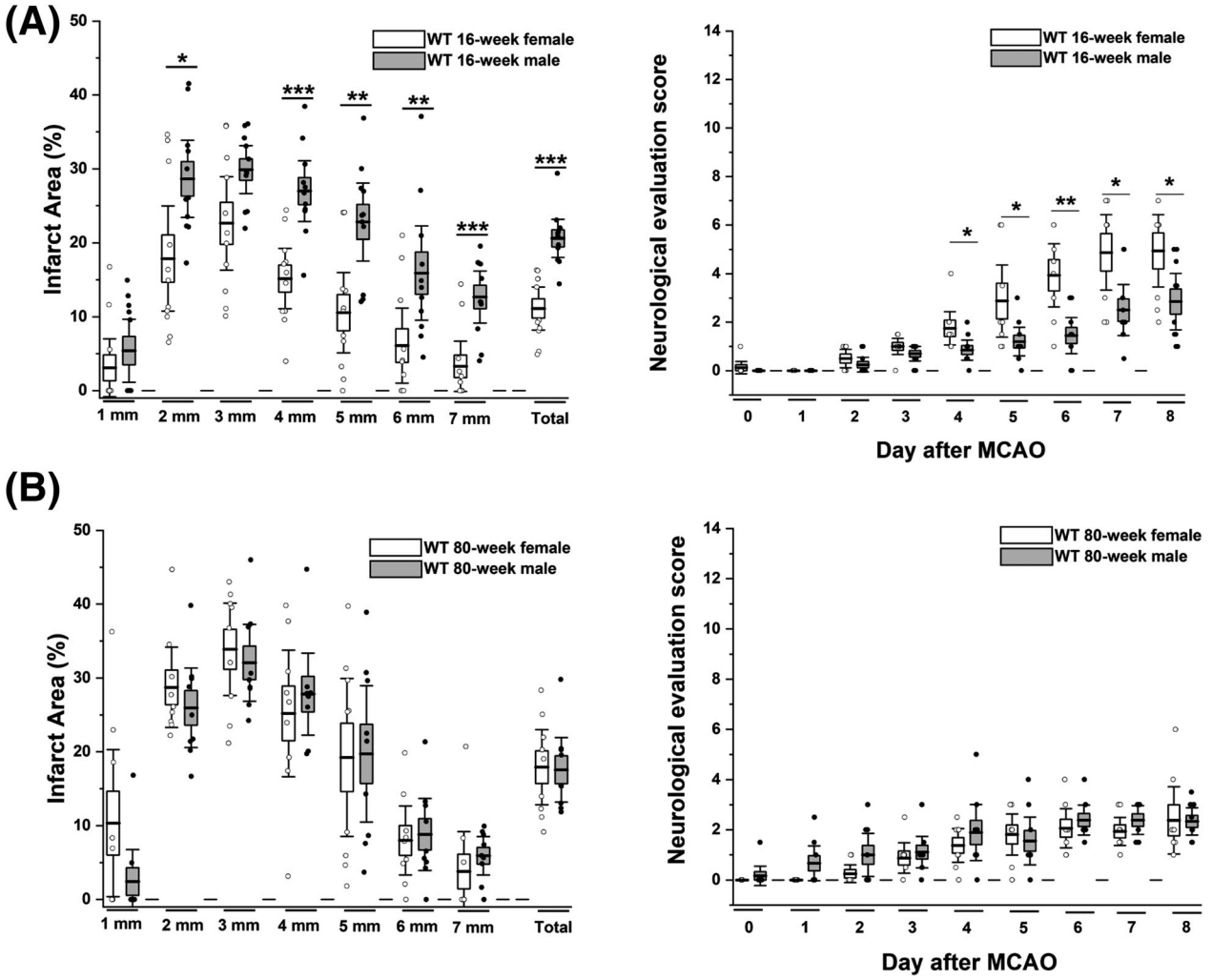

Figure 1. Comparison of stroke severity in young and old female versus male mice. Percent of infarcted hemisphere area was determined by T2-weighted MRI on day 8 after daily neurological deficit scoring. (A) Infarct area and deficit score in 16-week-old female (n = 11) were compared to male (n = 10) mice ($p < 0.001$ for infarct, $p = 0.029$ for NES). (B) Infarct area and deficit score in 80-week-old female (n = 9) were compared to male (n = 9) mice ($p = 0.623$ for infarct, $p = 0.446$ for NES). Data are shown as whisker plots with data overlay. The boxes show mean ± SEM and the whiskers show confidence intervals.

smaller infarcts than WT males, but if the percentages of Iba-1^+ and $CD3^+$ cells are ratioed to the infarct area, there is no significant, qualitative difference in the composition of the inflammation in males and females. Both sexes exhibited a similar density of microglia/macrophages and T cells in the infarct (Fig. S4). In 80-week-old female mice, we observed strong Kv1.3 staining in the infarcted hemisphere which localized to both Iba-1^+ hypertrophic microglia/macrophages and smaller $CD3^+$ T cells in immunofluorescence (Fig. 2A and B, white arrowheads). Based on observing Kv1.3 expression in females and thus confirming our previous findings in males, we hypothesized that aged animals of both sexes would benefit from Kv1.3 manipulation following ischemic stroke.

Genetic Kv1.3 deletion reduces infarction in young and old mice of both sexes, but is particularly effective in old females

We had previously found that Kv1.3 blockade reduced infarction in young male C56BL/6J mice and Wistar rats.[23] In order to more broadly assess the pathophysiological role of Kv1.3 in ischemic stroke we here evaluated the impact of Kv1.3 deficiency on stroke outcomes in both young and old, male and female mice. In 16-week-old male mice, Kv1.3 deletion reduced T2-weighted lesion area and improved neurological deficit score on day 8 compared to wild-type animals (Fig. 3A). In contrast, 16-week-old Kv1.$3^{-/-}$ female mice showed no significant

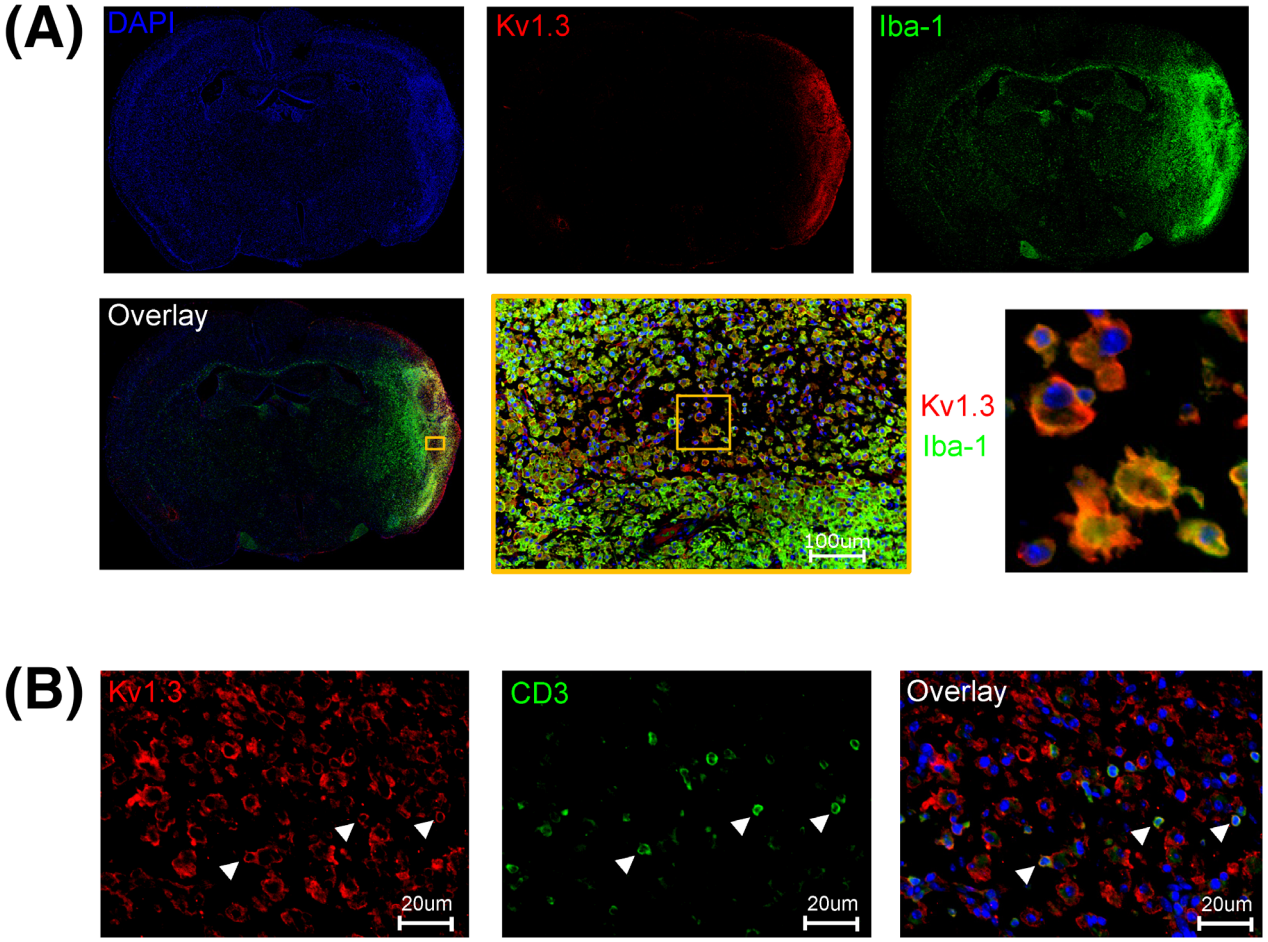

Figure 2. Kv1.3 is expressed on microglia/macrophages and T cells in the infarct of an 80-week-old female mouse. (A) Sample immunofluorescence staining of 5-μm thick paraffin sections from the 6-mm slice of an 80-week-old female mouse on day 8 after tMCAO. (A) Kv1.3 staining colocalizes to Iba-1$^+$ cells. (B) Kv1.3 staining on smaller, CD3$^+$ T cells (white arrowheads).

improvement in infarction or neurological deficit score on day 8 after MCAO (Fig. 3B).

When we next performed tMCAO surgeries in 80-week-old Kv1.3$^{-/-}$ mice, we observed an increased 8-day survival rate (80% vs. 75% for Kv1.3$^{-/-}$ males vs. WT males; 85.7% vs. 71.4% for females) as well as a significant reduction in T2-weighted lesion area on day 8, and an improvement in neurological deficits in both sexes compared to age-matched wild-type mice (Fig. 3C and D). These effects were particularly impressive in old females. Body weights for all groups are provided in Figure 4; infarct areas and neurological evaluation score (NES) for all groups on day 8 are provided in Table S1.

Treatment with the Kv1.3 blocker PAP-1 as a cytoprotectant started 12 h after reperfusion benefits both young and old female mice

Since the beneficial effects of Kv1.3 deletion on outcomes in tMCAO suggested that Kv1.3 could constitute a therapeutic target for immunocytoprotection after mechanical

Figure 3. Comparison of stroke severity in WT versus Kv1.3$^{-/-}$ mice. (A) Infarct area and deficit score in 16-week-old WT (n = 10) were compared to Kv1.3$^{-/-}$ (n = 14) male mice ($p < 0.001$ for infarct, $p = 0.033$ for NES). (B) Infarct area and deficit score in 16-week-old WT (n = 11) were compared to Kv1.3$^{-/-}$ (n = 14) female mice ($p = 0.058$ for infarct, $p = 0.551$ for NES). (C) Infarct area and deficit score in 80-week-old WT (n = 9) were compared to Kv1.3$^{-/-}$ (n = 12) male mice ($p = 0.056$ for infarct, $p < 0.001$ for NES). (D) Infarct area and deficit score in 80-week-old WT (n = 9) were compared to Kv1.3$^{-/-}$ (n = 18) female mice ($p = 0.001$ for infarct, $p < 0.001$ for NES). Data are shown as whisker plots with data overlay. The boxes show mean ± SEM and the whiskers show confidence intervals.

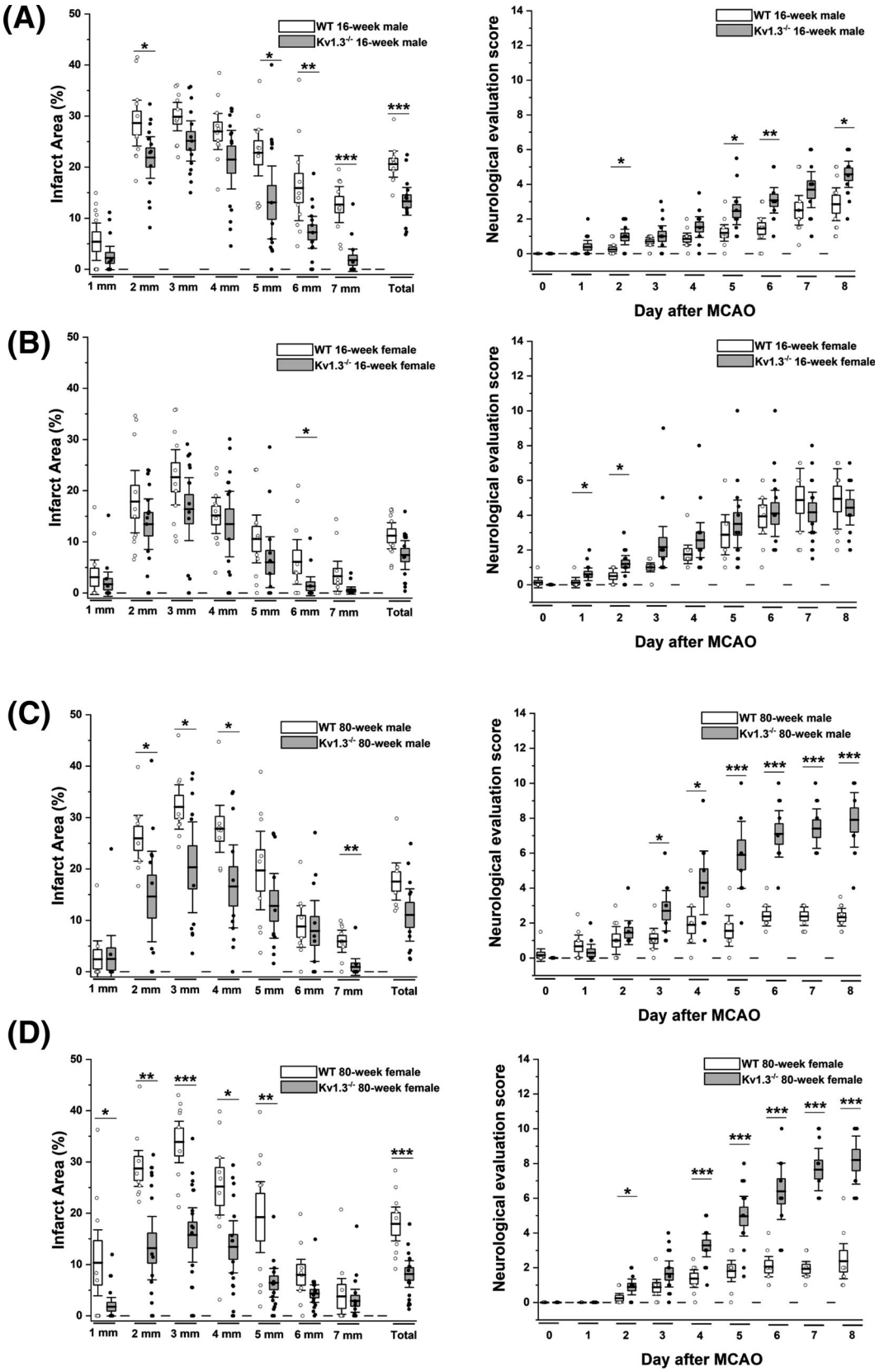

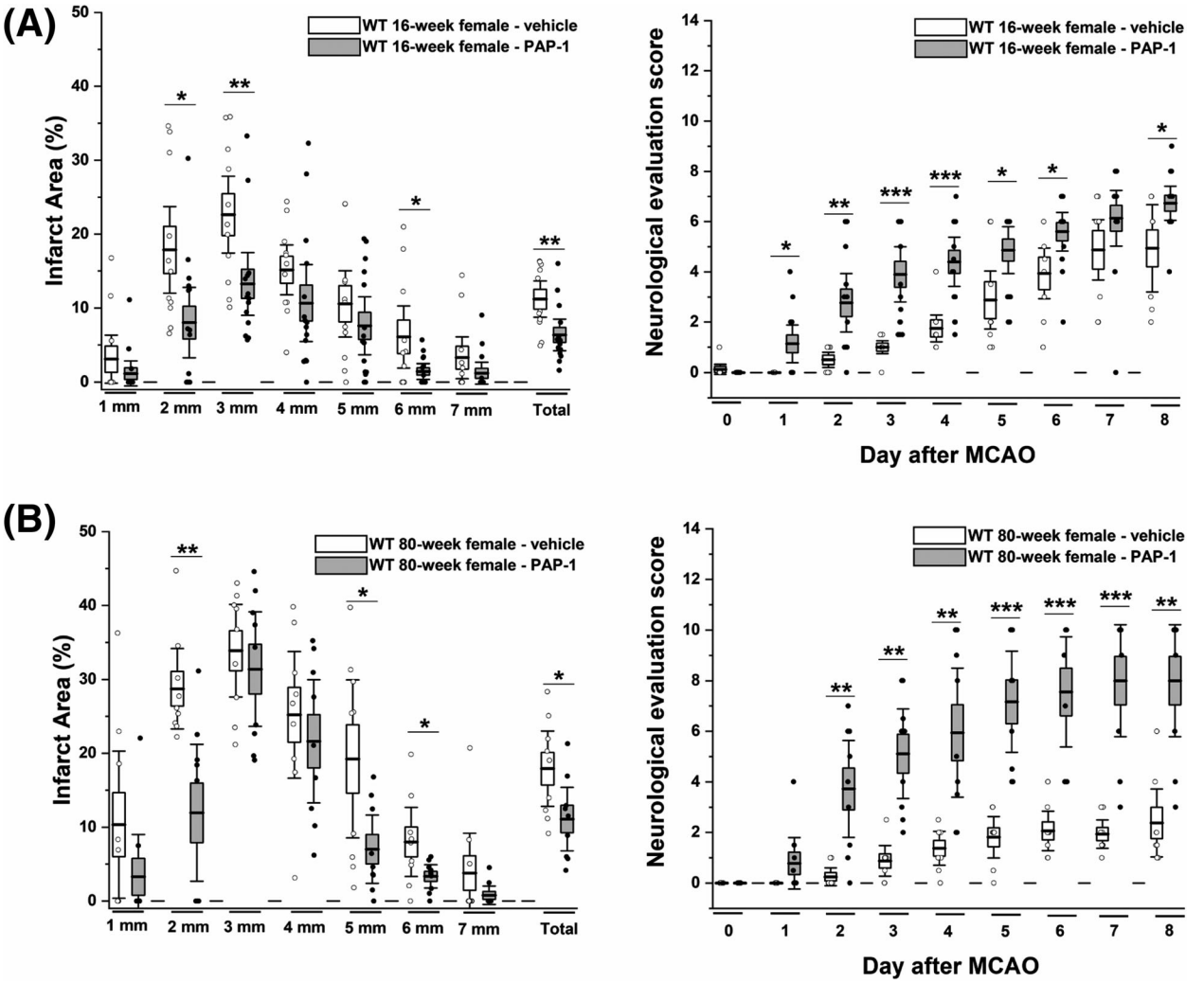

Figure 4. The Kv1.3 blocker PAP-1 reduces infarction and improves neurological deficit in young and old WT female mice. (A) Infarct area and deficit score in vehicle (n = 11) were compared to PAP-1 (40 mg/kg; n = 15) treated 16-week-old female mice (p = 0.007 for infarct, p = 0.016 for NES). (B) Infarct area and deficit score in vehicle (n = 9) were compared to PAP-1 (40 mg/kg; n = 9) treated 80-week-old female mice (p = 0.032 for infarct, p = 0.003 for NES). Data are shown as whisker plots with data overlay. The boxes show mean ± SEM and the whiskers show confidence intervals.

thrombectomy, we next treated 16-week-old and 80-week-old female mice twice daily with the Kv1.3 blocker PAP-1. This small molecule, which was developed in our laboratory, inhibits Kv1.3 with an IC_{50} of 2 nmol/L, exhibits good to excellent selectivity over other potassium channels as well as common receptors and transporter, and has undergone IND enabling toxicity studies for psoriasis without any concerning findings.[13,28] PAP-1 penetrates well into the brain and pharmacokinetic studies have shown that total brain concentrations equal plasma concentrations (C_{brain}/C_{plasma} = 1.1).[13,17]

In order to simulate a scenario with a long delay to adjunctive therapy after thrombectomy, PAP-1 administration was started 12 h after reperfusion and subsequent to the first neurological evaluation after the surgery where mice typically exhibit a score of ~1 in the DeRyck 14-score tactile and proprioceptive limp placing test.[29] In both young and old female mice, PAP-1 treatment (40 mg/kg i.p.) reduced T2-weighted lesion area on day 8 and improved neurological deficits (Fig. 4A and B) in comparison to vehicle-treated animals.

Kv1.3 blockade with PAP-1 or Kv1.3 deletion reduce microglia/macrophage activation and T-cell infiltration in old female mice

In order to access if the improvements we had observed in most groups with either Kv1.3 deletion or PAP-1

treatment were indeed accompanied by a reduction in neuroinflammation, we quantified Iba-1 and CD3 staining in the ipsilateral hemisphere in paraffin sections cut at 4 and 6 mm from the frontal pole in all animals from the three 80-week-old female groups (vehicle-treated WT, PAP-1-treated WT, and Kv1.3$^{-/-}$ mice) in an unbiased,

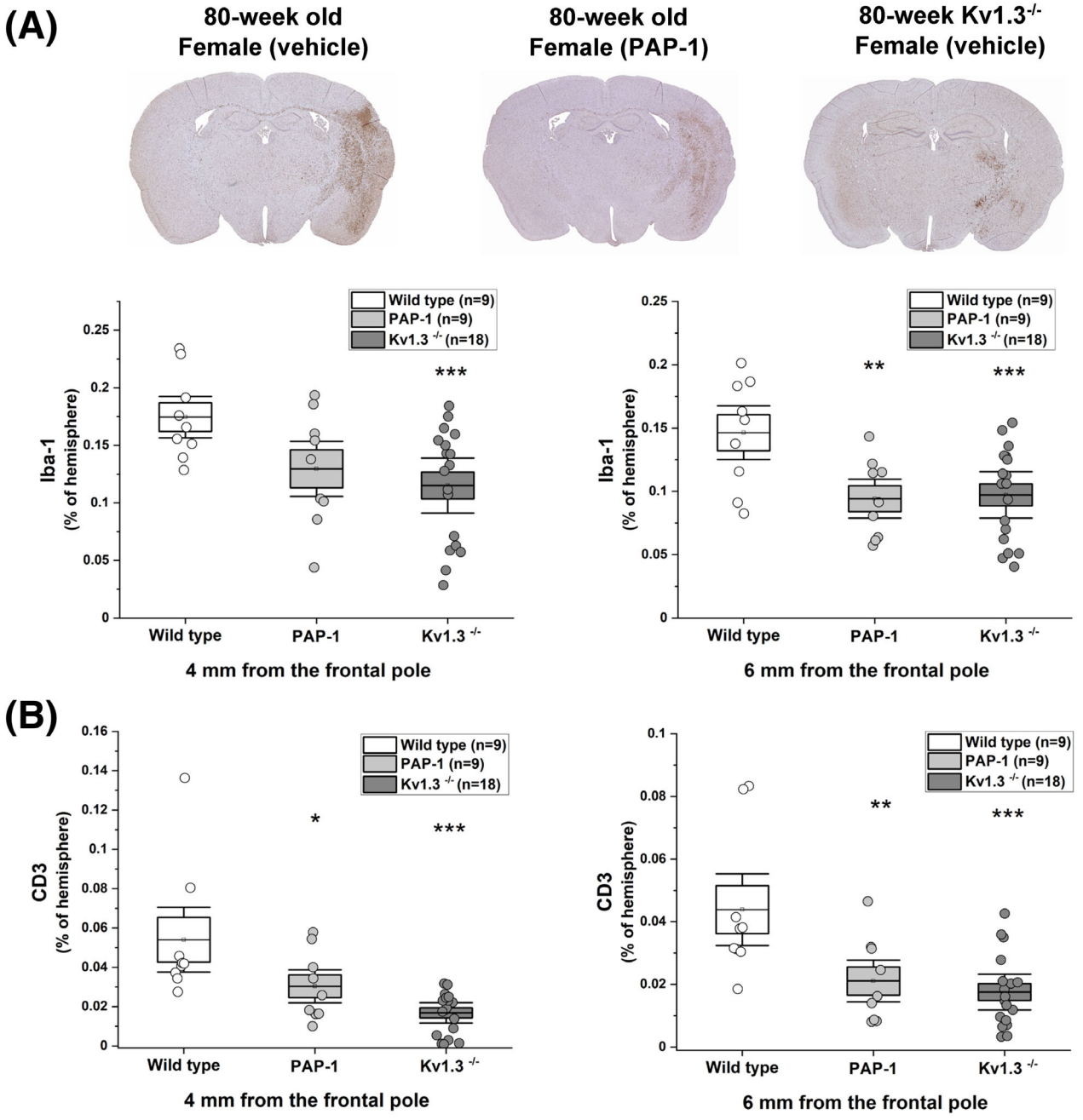

Figure 5. PAP-1 treatment and Kv1.3 deletion reduce Iba-1 and CD3 staining in 80-week-old female mice. Serial paraffin sections (5 μm thick) cut at 4 mm and the 6 mm from 80-week-old female mice were stained for Iba-1 and CD3. (A) Percentage of Iba-1-positive pixels in the infarcted hemisphere. Vehicle-treated WT (n = 9), PAP-1-treated WT (n = 9, p = 0.120 for 4-mm section; p = 0.014 for 6-mm section), and Kv1.3$^{-/-}$ (n = 18, p = 0.011 for 4-mm section; p = 0.007 for 6-mm section). (B) Percentage of CD3-positive pixels in the infarcted hemisphere. Vehicle-treated WT (n = 9), PAP-1-treated WT (n = 9, p = 0.049 for 4-mm section; p = 0.027 for 6-mm section), and Kv1.3$^{-/-}$ (n = 18, p < 0.001 for 4-mm section; p = 0.002 for 6-mm section). Data are shown as whisker plots with individual data overlay. The boxes show mean ± SEM and the whiskers show confidence intervals.

automated, pixel-based fashion (Fig. 5A and B). PAP-1 treatment and Kv1.3 deletion significantly reduced Iba-1-staining intensity which on day 8 captures both activated and proliferating microglia as well as infiltrating monocyte-derived macrophages (Fig. 5A). Both manipulations also profoundly reduced T-cell infiltration (Fig. 5B).

Discussion

Kv1.3 regulates membrane potential in T cells, monocyte-derived macrophages, and microglia.[12,33] By resisting depolarization during cellular activation, Kv1.3 channels enhance store-operated calcium influx as well as calcium influx through P2X4 receptors and fine tune downstream activation of the transcription factors NFAT in T cells and NFkB in microglia.[32–34] Kv1.3 expression is upregulated in effector memory T cells in humans and rodents,[13] in LPS-stimulated mouse microglia,[14] and in activated microglia in humans and rodent models of stroke, multiple sclerosis, Alzheimer's disease (AD), and Parkinson's disease.[17,18,23,35] A study using flow cytometry and transcriptomic profiling reported that Kv1.3^{high} microglia in postmortem AD brain and 5xFAD mice are CD11c^{+} and co-express Kv1.3 with many pro-inflammatory, disease-associated microglial genes such as *Il1b*, *Tlr2*, *Ifit2*, *Ptgs2*, *Stat1*, *Csf1*, *Tspo*, and *Slc16a3*.[16] Based on the findings that Kv1.3 inhibitors reduce pathology and improve behavioral outcomes in the rodent models mentioned above, targeting Kv1.3^{high} microglia and T cells constitutes an attractive approach for the treatment of neuroinflammation associated with ischemic stroke and/or the reperfusion from EVT. However, we previously only tested this hypothesis in young male mice and rats, an approach that can provide proof-of-concept, but is of limited predictive translational value because the majority of strokes occur in patients over 65 and, when considering overall lifetime risk, in females. While premenopausal women have a lower risk of stroke than men, this epidemiology reverses with age and in 2017 women accounted for 58% of US stroke deaths.[1] Based on the STAIR X recommendations for preclinical testing,[2] we therefore here evaluated both genetic Kv1.3 deletion and pharmacological Kv1.3 blockade with PAP-1 in aged and female mice.

C57BL/6J mice, the most commonly used inbred strain for stroke studies and the background strain for the Kv1.3$^{-/-}$ mice are considered mature adults at 3–6 months, middle aged at 10–14 months, and old at 18–24 months corresponding to 56–69 years in human age equivalents.[36] Natural survival then drops to below 50% at 28 months of age. To simulate young (~25 years) and old (~60 years) humans, but still have an acceptable surgical survival of >70% and be able to go out to the peaks of inflammation and Kv1.3 expression on day 8 after MCAO,[23] we here chose 16-week (=3.7 months) and 20-week (=18.5 months) old male and female mice. Female mice become sexually mature at 6 weeks and cycle until approximately 14 months of age.[31] The 80-week-old females used in this study were therefore acyclic and postmenopausal, consistent with our findings that 80-week-old WT males and females exhibited similar sized infarcts and comparable neurological impairment, while 16-week-old females had significantly smaller infarcts than old females and were better at recovering sensorimotor coordination. Young males, in contrast, did not perform better than old males in our hands and exhibited infarcts and neurological deficit scores that did not significantly differ from old males. Kv1.3 deletion ameliorated stroke outcomes in all groups with the exception of young females, which did not significantly benefit presumably because of their smaller infarcts due to the protective effects of estrogen in these cycling females.[31] PAP-1 treatment at the same 40 mg/kg dose that we had previously used in young male mice and found to be more effective than 10 mg/kg[23] reduced infarct area and improved sensorimotor coordination in old females as effectively as Kv1.3 deletion benefited old males and females. PAP-1 treatment at this dose also improved infarction in young females but had a less pronounced effect on neurological deficit than in old females. We suspect that the differences we observed between young male and young female mice for both genetic deletion and pharmacological blockade of Kv1.3 are largely due to the presence of estrogen which is known to reduce infarction in young females compared to young males and ovariectomized females.[31] In future studies it therefore would be interesting to investigate if Kv1.3 inhibition or deletion is more effective in ovariectomized females. However, since this study was powered to detect a relatively large 40% reduction in mean percentage infarct area with 80% power, it is also possible that we were underpowered to detect smaller improvements in young females. The later might be the case since we observed improvements with PAP-1 treatment in young WT females with a slightly larger group size. But one could also speculate that global lack of Kv1.3 induces a compensation in the immune system that counterbalances possible improvements in young females in the presence of estrogen.

Taken together, our results show that Kv1.3 deletion or pharmacological blockade improve outcomes in tMCAO on day 8 in females and in aged animals. Concerning sex, these findings are in line with our previous observations that there are no sex differences in functional Kv1.3 expression in cultured or acutely isolated mouse microglia[32] or in human T cells,[13] and that Kv1.3 inhibitors

have been widely found to be effective in female rats when used in autoimmune disease models such as experimental autoimmune encephalomyelitis, rheumatoid arthritis, or autoimmune diabetes.[13,37] We were, however, pleasantly surprised to observe improvements in stroke outcomes in aged mice, especially in neurological deficits score, with both genetic deletion and PAP-1 treatment initiated 12 h after reperfusion. These findings should of course be independently reproduced by another laboratory like our findings in young male rats recently were,[38] but could suggest a bigger contribution of Kv1.3^{high} microglia and T cells to stroke pathophysiology in aged animals. CD11c^{+} microglia, which express high levels of Kv1.3,[16] have recently been described to drive secondary, neurodegenerative changes in the thalamus after cortical strokes.[39] Regarding T cells, old C57BL/6 mice of both sexes recruit significantly more T cells into the brain than young and middle-aged mice following 60-min tMCAO[31] and CD4 T-cell depletion has been shown to improve behavioral outcomes on day-7 post-MCAO in aged mice without reducing infarct size.[40] There are further reports that brain-resident memory CD8 T cells, which appear to regulate microglia homeostasis under normal conditions, potentiate inflammation following ischemic injury by producing inflammatory cytokines and driving cytotoxic responses.[41,42] Considering these findings, we would like to posit that what makes targeting Kv1.3 effective in ischemic stroke in aged animals are the combined suppressive effects of Kv1.3 inhibition on pro-inflammatory, disease-associated microglia and on CD4^{+} and CD8^{+} memory T cells. Kv1.3 inhibition therefore could be considered to fulfill the requirement of being "pleiotropic" in the sense of targeting multiple effectors in the ischemic cascade as proposed for useful immunocytoprotectants for combination with EVT.[2] Increasing T-cell contribution to stroke pathophysiology has been proposed to be part of what is termed "inflammaging," a chronic low-grade inflammation accompanied by a shrinking of the naïve T-cell compartment and increase in terminally differentiated effector memory T cells with increased tissue homing capacity.[42]

How could our findings be further translated? We here started PAP-1 administration at 12 h after reperfusion. Future studies should explore earlier and later time windows for starting Kv1.3-targeted therapies and it should be evaluated whether Kv1.3 inhibition continues to provide benefit at longer time intervals after tMCAO. The pharmacological tool compound we used here, PAP-1, has undergone IND-enabling toxicity studies for psoriasis and could potentially be used in humans. Several new Kv1.3 inhibitors are also currently in preclinical development[43] and could become available for combination with EVT.

Conflict of Interest

H.W. is an inventor on a University of California patent claiming PAP-1 for immunosuppression. This patent has been abandoned because of its short remaining patent life.

Author Contributions

YJC and HW developed the concept and designed the study. YJC performed all surgeries. LS synthesized PAP-1. YJC and YC acquired and analyzed the data. YJC, YC, and HW prepared the figures. YJC and HW wrote the manuscript with input from all co-authors.

References

1. Virani SS, Alonso A, Benjamin EJ, et al. Heart disease and stroke statistics-2020 update: a report from the American Heart Association. Circulation. 2020;141:e139-e596.
2. Savitz SI, Baron J-C, Fisher M; Consortium SX. Stroke treatment academic industry roundtable X: brain cytoprotection therapies in the reperfusion era. Stroke. 2019;50:1026-1031.
3. Goyal M, Menon BK, van Zwam WH, et al. Endovascular thrombectomy after large-vessel ischaemic stroke: a meta-analysis of individual patient data from five randomised trials. Lancet. 2016;387:1723-1731.
4. Albers GW, Marks MP, Kemp S, et al. Thrombectomy for stroke at 6 to 16 hours with selection by perfusion imaging. N Engl J Med. 2018;378:708-718.
5. Wood H. Stroke: expanding the thrombectomy time window after stroke. Nat Rev Neurol. 2018;14:128.
6. Baron JC. Protecting the ischaemic penumbra as an adjunct to thrombectomy for acute stroke. Nat Rev Neurol. 2018;14:325-337.
7. Savitz SI, Baron J-C, Yenari MA, Sanossian N, Fisher M. Reconsidering neuroprotection in the reperfusion era. Stroke. 2017;48:3413-3419.
8. Iadecola C, Anrather J. The immunology of stroke: from mechanisms to translation. Nat Med. 2011;17:796-808.
9. Hu X, Li P, Guo Y, et al. Microglia/macrophage polarization dynamics reveal novel mechanism of injury expansion after focal cerebral ischemia. Stroke. 2012;43:3063-3070.
10. Kawabori M, Yenari MA. The role of the microglia in acute CNS injury. Metabol Brain Dis. 2015;30:381-392.
11. Meisel C, Schwab JM, Prass K, Meisel A, Dirnagl U. Central nervous system injury-induced immune deficiency syndrome. Nat Rev Neurosci. 2005;6:775-786.
12. Feske S, Wulff H, Skolnik EY. Ion channels in innate and adaptive immunity. Ann Rev Immunol. 2015;33:291-353.
13. Beeton C, Wulff H, Standifer NE, et al. Kv1.3 channels are a therapeutic target for T cell-mediated autoimmune diseases. Proc Natl Acad Sci USA. 2006;103:17414-17419.

14. Nguyen HM, Grössinger EM, Horiuchi M, et al. Differential Kv1.3, KCa3.1, and Kir2.1 expression in "classically" and "alternatively" activated microglia. Glia. 2017;65:106-121.
15. Di Lucente J, Nguyen HM, Wulff H, et al. The voltage-gated potassium channel Kv1.3 is required for microglial pro-inflammatory activation in vivo. Glia. 2018;66:1881-1895.
16. Ramesha S, Rayaprolu S, Bowen CA, et al. Unique molecular characteristics and microglial origin of Kv1.3 channel-positive brain myeloid cells in Alzheimer's disease. Proc Natl Acad Sci USA. 2021;118(11):e2013545118.
17. Maezawa I, Nguyen HM, Di Lucente J, et al. Kv1.3 inhibition as a potential microglia-targeted therapy for Alzheimer's disease: preclinical proof-of-concept. Brain. 2018;141:596-612.
18. Sarkar S, Nguyen HM, Malovic E, et al. Kv1.3 modulates neuroinflammation and neurodegeneration in Parkinson's disease. J Clin Invest. 2020;130:4195-4212.
19. Lai IK, Valdearcos M, Morioka K, et al. Blocking Kv1.3 potassium channels prevents postoperative neuroinflammation and cognitive decline without impairing wound healing in mice. Br J Anaesth. 2020;25:298-307.
20. Tarcha EJ, Olsen CM, Probst P, et al. Safety and pharmacodynamics of dalazatide, a Kv1.3 channel inhibitor, in the treatment of plaque psoriasis: a randomized phase-1b trial. PLoS One. 2017;12(7):e0180762.
21. Pereira LE, Villinger F, Wulff H, Sankaranarayanan A, Raman G, Ansari AA. Pharmacokinetics, toxicity, and functional studies of the selective Kv1.3 channel blocker 5-(4-phenoxybutoxy)psoralen in rhesus macaques. Exp Biol Med. 2007;232:1338-1354.
22. Matheu MP, Beeton C, Garcia A, et al. Imaging of effector memory T cells during a delayed-type hypersensitivity reaction and suppression by Kv1.3 channel block. Immunity. 2008;29:602-614.
23. Chen Y-J, Nguyen HM, Maezawa I, Jin L-W, Wulff H. Inhibition of the potassium channel Kv1.3 reduces infarction and inflammation in ischemic stroke. Ann Clin Transl Neurol. 2018;5:147-161.
24. Sutherland BA, Neuhaus AA, Couch Y, et al. The transient intraluminal filament middle cerebral artery occlusion model as a model of endovascular thrombectomy in stroke. J Cereb Blood Flow Metab. 2016;36:363-369.
25. Percie du Sert N, Alfieri A, Allan SM, et al. The IMPROVE guidelines (Ischaemia Models: Procedural Refinements of in Vivo Experiments). J Cereb Blood Flow Metab. 2017;37:3488-3517.
26. Koni PA, Khanna R, Chang MC, et al. Compensatory anion currents in Kv1.3 channel-deficient thymocytes. J Biol Chem. 2003;278:39443-39451.
27. Longa EZ, Weinstein PR, Carlson S, Cummins R. Reversible middle cerebral artery occlusion without craniectomy in rats. Stroke. 1989;20:84-91.
28. Schmitz A, Sankaranarayanan A, Azam P, et al. Design of PAP-1, a selective small molecule Kv1.3 blocker, for the suppression of effector memory T cells in autoimmune diseases. Mol Pharmacol. 2005;68:1254-1270.
29. De Ryck M, Van Reempts J, Borgers M, Wauquier A, Janssen PA. Photochemical stroke model: flunarizine prevents sensorimotor deficits after neocortical infarcts in rats. Stroke. 1989;20:1383-1390.
30. Schlattmann P, Dirnagl U. Statistics in experimental cerebrovascular research: comparison of more than two groups with a continuous outcome variable. J Cereb Blood Flow Metab. 2010;30:1558-1563.
31. Manwani B, Liu F, Scranton V, Hammond MD, Sansing LH, McCullough LD. Differential effects of aging and sex on stroke induced inflammation across the lifespan. Exp Neurol. 2013;249:120-131.
32. Nguyen HM, di Lucente J, Chen Y-J, et al. Biophysical basis for Kv1.3 regulation of membrane potential changes induced by P2X4-mediated calcium entry in microglia. Glia. 2020;68:2377-2394.
33. Fomina AF, Nguyen HM, Wulff H. Kv1.3 inhibition attenuates neuroinflammation through disruption of microglial calcium signaling. Channels. 2021;15:67-78.
34. Negulescu PA, Shastri N, Cahalan MD. Intracellular calcium dependence of gene expression in single T lymphocytes. Proc Natl Acad Sci USA. 1994;91:2873-2877.
35. Rus H, Pardo CA, Hu L, et al. The voltage-gated potassium channel Kv1.3 is highly expressed on inflammatory infiltrates in multiple sclerosis brain. Proc Natl Acad Sci USA. 2005;102:11094-11099.
36. Flurkey K, Currer JM, Harrison DE. The mouse in aging research. In: Fox JG, ed. The Mouse in Biomedical Research. 2nd ed. Elsevier; 2007:637-672.
37. Tarcha EJ, Chi V, Munoz-Elias EJ, et al. Durable pharmacological responses from the peptide drug ShK-186, a specific Kv1.3 channel inhibitor that suppresses T cell mediators of autoimmune disease. J Pharmacol Exp Ther. 2012;342:642-653.
38. Ma DC, Zhang NN, Zhang YN, Chen HS. Kv1.3 channel blockade alleviates cerebral ischemia/reperfusion injury by reshaping M1/M2 phenotypes and compromising the activation of NLRP3 inflammasome in microglia. Exp Neurol. 2020;332:113399.
39. Cao Z, Harvey SS, Chiang T, et al. Unique subtype of microglia in degenerative thalamus after cortical stroke. Stroke. 2021;52:687-698.
40. Harris NM, Roy-O'Reilly M, Ritzel RM, et al. Depletion of CD4 T cells provides therapeutic benefits in aged mice after ischemic stroke. Exp Neurol. 2020;326:113202.
41. Ritzel RM, Crapser J, Patel AR, et al. Age-associated resident memory CD8 T cells in the central nervous system are primed to potentiate inflammation after ischemic brain injury. J Immunol. 2016;196:3318-3330.

42. Carrasco E, Gómez de las Heras MM, Gabandé-Rodríguez E, Desdín-Micó G, Aranda JF, Mittelbrunn M. The role of T cells in age-related diseases. Nat Rev Immunol. 2021;16:2989–3001.
43. Unterweger AL, Jensen MO, Giordanetto F, et al. Suppressing Kv1.3 ion channel activity with a novel small molecule inhibitor ameliorates inflammation in a humanized mouse model of ulcerative colitis. J Crohns Colitis. 2021:jjab078. https://doi.org/10.1093/ecco-jcc/jjab078. Online ahead of print.

Supporting Information

Additional supporting information may be found online in the Supporting Information section at the end of the article.

Table S1. Total infarct area and neurological deficit score on day-8 after MCAO in all animal groups.

Figure S1. Body weight evolution in young and old male and female C57BL/6J mice after tMCAO surgery. Shown are daily body weights before and for 8 days after 60 min of tMCAO in 16-week-old female ($n = 11$) and male ($n = 10$) mice (*Left*), and 80-week-old female ($n = 9$) and male ($n = 9$) male mice. Data are shown as whisker plots with induvial data overlay. The boxes show mean ± SEM and the whiskers show confidence intervals.

Figure S2. Comparison of stroke severity in young versus old animals of the same sex. Please note that this is the same data as in Figure 1 of the main text, but here we are comparing percent of infarcted hemisphere area as determined by T2-weighted MRI on day 8 and daily neurological deficit scoring between 16-week-old females ($n = 11$) and 80-week-old females ($n = 9$) [$p = 0.016$ for infarct, $p = 0.003$ for NES], and between 16-week-old males ($n = 10$) and 80-week-old males ($n = 9$) [$p = 0.211$ for infarct, $p = 0.393$ for NES]. Data are shown as whisker plots with individual data overlay. The boxes show mean ± SEM and the whiskers show confidence intervals.

Figure S3. Intense Kv1.3 staining is observed in the infarcted area in both sexes. Heterozygous male and female $CX3CR1^{+/GFP}$ mice, which express GFP (green fluorescent protein) instead of one copy of CX3CR1 in microglia, macrophages, and dendritic cells, were used for tMCAO surgery. On day 8, animals were sacrificed and 14-μm thick cryosections were stained with a polyclonal rabbit anti-Kv1.3 antibody (Alomone, APC-101, 1:1000) followed by an Alexa Fluor®546-conjugated secondary antibody (1:1000, Life Technologies). Please note that $CX3CR1^{+/GFP}$ mice were only used for immunohistochemistry but not for any treatment experiments because of their lack of one copy of CX3CR1.

Figure S4. Comparison of the composition of immune cell infiltrate in 16-week-old male and female C57BL/6J mice on day 8 after tMCAO. Serial paraffin sections (5-μm thick) cut at 4 and 6 mm from the frontal pole from male and female mice were stained for Iba-1 and CD3 as described in the method section of the main text. Positive pixels were ratioed to the infarcted area and not to the hemisphere area to account for the smaller infarcts in young females. Data are shown as whisker plots with individual data overlay. The boxes show mean ± SEM and the whiskers show confidence intervals.

Figure S5. Body weight evolution in WT versus $Kv1.3^{-/-}$ mice or versus PAP-1-treated mice after tMCAO surgery. Shown are daily body weights before and for 8 days after 60 min of tMCAO. (A) Body weights in 16-week-old male WT mice ($n = 10$) versus male $Kv1.3^{-/-}$ mice ($n = 14$), and in 16-week-old female WT ($n = 11$) versus female $Kv1.3^{-/-}$ mice ($n = 14$). (B) Body weights in 80-week-old male WT mice ($n = 9$) versus male $Kv1.3^{-/-}$ mice ($n = 12$), and in 80-week-old female WT ($n = 9$) versus female $Kv1.3^{-/-}$ mice ($n = 18$). (C) Body weights in 16-week-old female WT mice ($n = 11$) versus female WT mice treated with 40 mg/kg of PAP1 ($n = 15$), and body weights in 80-week-old female WT mice ($n = 9$) versus female WT mice treated with 40 mg/kg PAP-1 ($n = 9$). Data are shown as whisker plots with individual data overlay. The boxes show mean ± SEM and the whiskers show confidence intervals.

